Mathematical Modelling and Numerical Analysis ESAIM: M2AN
Modélisation Mathématique et Analyse Numérique Vol. 35, N° 3, 2001, pp. 595–605

CRACK DETECTION USING ELECTROSTATIC MEASUREMENTS *

Martin Brühl[1], Martin Hanke[1] and Michael Pidcock[2]

Abstract. In this paper we extend recent work on the detection of inclusions using electrostatic measurements to the problem of crack detection in a two-dimensional object. As in the inclusion case our method is based on a factorization of the difference between two Neumann-Dirichlet operators. The factorization possible in the case of cracks is much simpler than that for inclusions and the analysis is greatly simplified. However, the directional information carried by the crack makes the practical implementation of our algorithm more computationally demanding.

Mathematics Subject Classification. 35R30, 31A25.

Received: July 25, 2000.

Introduction

In non-destructive testing an important area of research is the detection of cracks within the material being investigated. There are a wide variety of methods that are used to solve this problem but most devices exploit one of two basic approaches. The first type use acoustic or electromagnetic scattering data while the second use elastostatic or electrostatic measurements made on the surface of the object.

In this work we consider the use of electrostatic measurements following in this way the landmark paper of Friedman and Vogelius [6]: We assume that a set of electrodes is attached to the surface of an object and that these electrodes inject a sequence of independent currents into the body. Ignoring some technical difficulties we shall also assume that the same electrodes can be used to obtain measurements of the resulting surface potential. In mathematical terms the potential is the solution of an elliptic boundary value problem, and the known boundary data correspond to some partial knowledge of the Neumann-Dirichlet map for the associated differential operator. To detect cracks we have to determine from these data essential features of the diffusion coefficient in the differential operator. This is an inverse boundary value problem.

Our approach to solving this inverse problem is based on the assumption that the body is homogeneously conducting, except for the cracks, which are insulating. For ease of simplicity we restrict ourselves to two space dimensions in which case a crack is an arc.

We propose a numerical algorithm for reconstructing the cracks from the given measurements which is non-iterative. This is quite different from most competing schemes, see for instance [4, 13, 14] and the references therein. In our algorithm we need to solve only one forward problem per boundary current, corresponding to

Keywords and phrases. Inverse boundary value problem, nondestructive testing, crack.

* *The research of the first author was supported by the Deutsche Forschungsgemeinschaft, grant HA 2121/2-3.*

[1] Fachbereich Mathematik, Johannes Gutenberg-Universität, 55099 Mainz, Germany. e-mail: bruehl@math.uni-mainz.de; e-mail: hanke@math.uni-mainz.de

[2] School of Computing and Mathematical Sciences, Oxford Brookes University, Oxford OX3 0BP, Great Britain. e-mail: mkpidcock@brookes.ac.uk

a homogeneous body without cracks. While it is known that only two currents suffice to identify any finite distribution of cracks (*cf.* [1, 7]), our method requires a moderate number of measurements in practice. We would like to emphasize, however, that the number of cracks need not be known *a priori*.

The method itself is an extension of an algorithm from [2, 3] for an inverse problem in electrical impedance tomography. This algorithm can be used to decide whether a given point within the body belongs to the interior of an insulating inclusion – it will not recognize points on the boundary as being part of the inclusion. In spite of the similarity of these two inverse problems, the crack problem causes new difficulties because cracks have empty interior. We therefore have to modify this algorithm to see cracks.

On the other hand, the subtle difference between the two inverse problems allows an alternative way to derive the theoretical basis of the algorithm in the crack context. This new analysis is shorter and much more elementary than the one in [2]. Although we currently do not see how to extend this new analysis to the impedance tomography problem we believe that the new technique deepens our understanding of the general case.

Historically, the method in [2] followed an approach by Kirsch [8] for certain inverse scattering problems. Kirsch's method also fails when it comes to detecting points on the boundary of the scattering obstacle. Recently Kirsch and Ritter [9] have therefore modified the algorithm from [8] to reconstruct cracks from the far-field pattern of scattering data. These modifications are similar to the one that we propose here. However, the theoretical derivation in [9] parallels the original one in [8], and is different in spirit from the one we give here. As far as we know, our new analysis does not yet have an appropriate analog in the inverse scattering context.

1. The forward problem

Consider a bounded, simply connected domain $\Omega \subset \mathbb{R}^2$ representing a homogeneously conducting object. Let $\Gamma = \partial\Omega$ be the sufficiently smooth boundary of Ω with outer normal ν on Γ.

In the absence of cracks the solution u of the boundary value problem

$$\Delta u = 0 \quad \text{in } \Omega, \qquad \frac{\partial u}{\partial \nu} = \begin{cases} f & \text{on } \Gamma_0, \\ 0 & \text{on } \Gamma \setminus \Gamma_0, \end{cases} \tag{1}$$

is the potential resulting from a boundary current with support on $\Gamma_0 \subset \Gamma$. We may think of Γ_0 as being the part of the boundary covered by electrodes. In order to guarantee solvability of (1) we need to assume that

$$f \in \mathrm{L}^2_\diamond(\Gamma_0) = \{f \in \mathrm{L}^2(\Gamma_0) : \int_{\Gamma_0} f \,\mathrm{d}s = 0\}.$$

We denote by

$$g = u|_{\Gamma_0} \in \mathrm{L}^2_\diamond(\Gamma_0) \tag{2}$$

the boundary values of the potential on Γ_0, where we impose the normalization in (2) to enforce uniqueness of the potential.

In the presence of insulating cracks, the boundary value problem (1) has to be modified. We define a *crack* $\sigma \subset \Omega$ to be a compact, simple arc (not a point) which is sufficiently smooth so that we can assign for each point $x \in \sigma$ a unit normal vector $n = n(x)$ varying smoothly over σ. We denote by $\Sigma \subset \Omega$ the collection of all cracks and assume that $\Omega \setminus \Sigma$ is connected. If Σ is not the empty set the same Neumann boundary condition as above yields a potential $\tilde{u}$ which solves the diffraction problem

$$\Delta \tilde{u} = 0 \quad \text{in } \Omega \setminus \Sigma, \qquad \frac{\partial \tilde{u}}{\partial \nu} = \begin{cases} f & \text{on } \Gamma_0, \\ 0 & \text{on } \Gamma \setminus \Gamma_0, \end{cases} \qquad \frac{\partial \tilde{u}}{\partial n} = 0 \quad \text{on } \Sigma. \tag{3}$$

The last condition in (3) expresses the fact that no current flows across Σ, *i.e.*, that the cracks are insulating; see Section 4 for the modifications to the theory necessary in the presence of perfectly conducting cracks.

More rigorously speaking, the solutions u and $\tilde{u}$ of (1) and (3) are defined in the variational sense

$$\int_\Omega \operatorname{grad} u \cdot \operatorname{grad} \phi \, \mathrm{d}x = \int_{\Gamma_0} f\phi \, \mathrm{d}s \qquad \text{for all } \phi \in \mathrm{H}^1_\diamond(\Omega), \tag{4}$$

and

$$\int_{\Omega\setminus\Sigma} \operatorname{grad} \tilde{u} \cdot \operatorname{grad} \tilde{\phi} \, \mathrm{d}x = \int_{\Gamma_0} f\tilde{\phi} \, \mathrm{d}s \qquad \text{for all } \tilde{\phi} \in \mathrm{H}^1_\diamond(\Omega \setminus \Sigma), \tag{5}$$

respectively. Here we denote by $\mathrm{H}^1_\diamond(\Omega)$ the subspace of the standard Sobolev space $\mathrm{H}^1(\Omega)$ consisting of only those $u \in \mathrm{H}^1(\Omega)$ with boundary values $u|_{\Gamma_0} \in \mathrm{L}^2_\diamond(\Gamma_0)$. The other space $\mathrm{H}^1_\diamond(\Omega \setminus \Sigma)$ is the closure of

$$\mathcal{C} = \{u \in \mathrm{C}^\infty(\overline{\Omega} \setminus \Sigma) : \int_{\Omega\setminus\Sigma} |\operatorname{grad} u|^2 \, \mathrm{d}x < \infty, \ \int_{\Gamma_0} u \, \mathrm{d}s = 0\}$$

with respect to the norm

$$\|u\| = \Big(\int_{\Omega\setminus\Sigma} |\operatorname{grad} u|^2 \, \mathrm{d}x\Big)^{1/2} \tag{6}$$

and its associated inner product

$$\langle u, v\rangle = \int_{\Omega\setminus\Sigma} \operatorname{grad} u \cdot \operatorname{grad} v \, \mathrm{d}x. \tag{7}$$

Note that (6) defines a norm in $\mathrm{H}^1_\diamond(\Omega)$ and $\mathrm{H}^1_\diamond(\Omega \setminus \Sigma)$ due to the constraint $\int_{\Gamma_0} u \, \mathrm{d}s = 0$.

A function $u \in \mathrm{H}^1_\diamond(\Omega \setminus \Sigma)$ may have different traces on either side of a crack and it belongs to $\mathrm{H}^1_\diamond(\Omega)$ if and only if these traces coincide for all cracks, respectively, *i.e.*, if the jump $[u]_\Sigma$ of u across Σ vanishes. The sign of the jump is implicitly fixed through the direction of the normal n such that Green's formula becomes

$$\int_{\Omega\setminus\Sigma} \operatorname{grad} v \cdot \operatorname{grad} w \, \mathrm{d}x = \int_\Gamma v \frac{\partial w}{\partial \nu} \, \mathrm{d}s + \int_\Sigma v \left[\frac{\partial w}{\partial n}\right]_\Sigma \mathrm{d}s - \int_{\Omega\setminus\Sigma} v\Delta w \, \mathrm{d}x,$$

valid for all $v \in \mathrm{H}^1_\diamond(\Omega)$ and all $w \in \mathcal{C}$ with $\Delta w \in \mathrm{L}^2(\Omega)$.

We shall now investigate the orthogonal complement of $\mathrm{H}^1_\diamond(\Omega)$ in $\mathrm{H}^1_\diamond(\Omega \setminus \Sigma)$.

Lemma 1.1. *The orthogonal complement $\mathcal{K}$ of $\mathrm{H}^1_\diamond(\Omega)$ in $\mathrm{H}^1_\diamond(\Omega\setminus\Sigma)$ with respect to the inner product* (7) *consists of all harmonic functions w in $\Omega \setminus \Sigma$ with*

$$\frac{\partial w}{\partial \nu} = 0 \quad \text{on } \Gamma \qquad \text{and} \qquad \left[\frac{\partial w}{\partial n}\right]_\Sigma = 0. \tag{8}$$

Proof. For $v \in \mathrm{H}^1_\diamond(\Omega)$ and a harmonic function $w \in \mathrm{H}^1_\diamond(\Omega \setminus \Sigma)$ Green's formula yields

$$\int_{\Omega\setminus\Sigma} \operatorname{grad} v \cdot \operatorname{grad} w \, \mathrm{d}x = \int_\Gamma v \frac{\partial w}{\partial \nu} \, \mathrm{d}s + \int_\Sigma v \left[\frac{\partial w}{\partial n}\right]_\Sigma \mathrm{d}s, \tag{9}$$

and hence $w \in \mathcal{K}$ if w satisfies the boundary conditions (8).

Conversely, if $w \in \mathcal{K}$ then

$$0 = \langle v, w \rangle = \int_{\Omega \setminus \Sigma} \operatorname{grad} v \cdot \operatorname{grad} w \, \mathrm{d}x$$

for every $v \in \mathrm{H}^1_\diamond(\Omega)$. It now follows from Weyl's Lemma that w is harmonic in $\Omega \setminus \Sigma$, and consequently that (9) is valid for every $v \in \mathrm{H}^1_\diamond(\Omega)$. Hence, w satisfies the desired boundary conditions on Γ and Σ in the usual weak sense. □

2. A factorization of the Neumann-Dirichlet operators

The mapping $\Lambda : \mathrm{L}^2_\diamond(\Gamma_0) \to \mathrm{L}^2_\diamond(\Gamma_0)$, which takes $f \in \mathrm{L}^2_\diamond(\Gamma_0)$ in (1) onto the respective g of (2) is called the *local Neumann-Dirichlet operator* associated with the Laplacian in Ω, since it maps the Neumann boundary values of a potential onto its Dirichlet values. Here the term 'local' refers to the fact that all information is restricted to $\Gamma_0 \subset \Gamma$. Similarly, the operator

$$\tilde{\Lambda} : \begin{cases} \mathrm{L}^2_\diamond(\Gamma_0) \longrightarrow \mathrm{L}^2_\diamond(\Gamma_0), \\ f \longmapsto \tilde{g} = \tilde{u}|_{\Gamma_0}, \end{cases}$$

is the local Neumann-Dirichlet operator associated with the boundary value problem (3).

In principle, it is possible to pursue the approach in [2] to derive a LDL^*-factorization of the difference between the two Neumann-Dirichlet operators

$$\tilde{\Lambda} - \Lambda = LDL^*, \tag{10}$$

where $L : \mathrm{L}^2_\diamond(\Sigma) \to \mathrm{L}^2_\diamond(\Gamma_0)$ and D is an unbounded selfadjoint and positive semidefinite linear operator on $\mathrm{L}^2_\diamond(\Sigma)$; here $\mathrm{L}^2_\diamond(\Sigma)$ is an appropriate closed subspace of $\mathrm{L}^2(\Sigma)$. Such a factorization was a basic ingredient in [2] in the characterization of the range of the square root operator $(\tilde{\Lambda} - \Lambda)^{1/2}$. A similar factorization has also been used in [9] in the scattering context to describe the range of the square root of the associated far field operator.

Here we shall use a different argument which evolves from a normal equation type factorization of $\tilde{\Lambda} - \Lambda$, *i.e.*, a factorization

$$\tilde{\Lambda} - \Lambda = K^* K, \tag{11}$$

where K has some natural meaning. As we shall see below, the existence of such a factorization greatly simplifies the characterization of the range $\mathcal{R}((\tilde{\Lambda} - \Lambda)^{1/2})$.

For the crack problem one factorization (11) is surprisingly simple. Given an input current $f \in \mathrm{L}^2_\diamond(\Gamma_0)$, define

$$K : \begin{cases} \mathrm{L}^2_\diamond(\Gamma_0) \longrightarrow \mathrm{H}^1_\diamond(\Omega \setminus \Sigma), \\ f \longmapsto \tilde{u} - u, \end{cases} \tag{12}$$

where u and $\tilde{u}$ are the potentials in (1) and (3). Then we immediately have $\tilde{\Lambda} - \Lambda = \gamma_0 K$, where

$$\gamma_0 : \begin{cases} \mathrm{H}^1_\diamond(\Omega \setminus \Sigma) \longrightarrow \mathrm{L}^2_\diamond(\Gamma_0), \\ v \longmapsto v|_{\Gamma_0}, \end{cases}$$

is the trace operator associated with Γ_0. It turns out (see Th. 2.1 below) that γ_0 and the adjoint of K coincide on $\mathcal{R}(K)$, and hence we have established (11).

Theorem 2.1. *The closure of $\mathcal{R}(K)$ coincides with the subspace $\mathcal{K}$ of Lemma* 1.1*, and the adjoint operator $K^* : \mathrm{H}^1_\diamond(\Omega \setminus \Sigma) \to \mathrm{L}^2_\diamond(\Gamma_0)$ of K is given by*

$$K^* v = \begin{cases} \gamma_0 v, & v \in \mathcal{K}, \\ 0, & v \in \mathrm{H}^1_\diamond(\Omega). \end{cases}$$

In particular, we have

$$\tilde{\Lambda} - \Lambda = \gamma_0 K = K^* K.$$

Proof. Let $w \in \mathcal{R}(K)$; then $w = Kf = \tilde{u} - u$ for some input current $f \in \mathrm{L}^2_\diamond(\Gamma_0)$ and corresponding potentials u and $\tilde{u}$ of (1) and (3), respectively. From the weak formulations (4) and (5) of these boundary value problems we obtain for arbitrary $\phi \in \mathrm{H}^1_\diamond(\Omega) \subset \mathrm{H}^1_\diamond(\Omega \setminus \Sigma)$,

$$\int_{\Omega\setminus\Sigma} \operatorname{grad} w \cdot \operatorname{grad} \phi \, \mathrm{d}x = \int_{\Omega\setminus\Sigma} \operatorname{grad}(\tilde{u} - u) \cdot \operatorname{grad} \phi \, \mathrm{d}x = 0,$$

because $|\operatorname{grad} \phi| \in \mathrm{L}^2(\Omega)$ and Σ has Lebesgue measure zero. This proves the orthogonality of $\mathcal{R}(K)$ and $\mathrm{H}^1_\diamond(\Omega)$, and hence, $\mathcal{R}(K) \subset \mathcal{K}$.

Next we determine K^*. Choosing $v \in \mathcal{K}$ we obtain for any input current $f \in \mathrm{L}^2_\diamond(\Gamma_0)$ and associated potentials $u \in \mathrm{H}^1_\diamond(\Omega)$ and $\tilde{u} \in \mathrm{H}^1_\diamond(\Omega \setminus \Sigma)$ of (1) and (3)

$$\langle Kf, v\rangle = \langle \tilde{u} - u, v\rangle = \langle \tilde{u}, v\rangle - \langle u, v\rangle = \langle \tilde{u}, v\rangle,$$

since $\langle u, v\rangle$ vanishes because of the orthogonality of $\mathcal{K}$ and $\mathrm{H}^1_\diamond(\Omega)$. From the weak definition (5) of $\tilde{u}$ we therefore obtain

$$\langle Kf, v\rangle = \int_{\Gamma_0} f v \, \mathrm{d}s,$$

and since this identity holds for any $f \in \mathrm{L}^2_\diamond(\Gamma_0)$ we conclude that $v|_{\Gamma_0} = \gamma_0 v$ equals $K^* v$, *i.e.*, $K^* = \gamma_0$ on $\mathcal{K}$. Moreover, since

$$\mathrm{H}^1_\diamond(\Omega) \subset \mathcal{R}(K)^\perp = \mathcal{N}(K^*) \tag{13}$$

we have $K^* = 0$ on $\mathrm{H}^1_\diamond(\Omega)$.

To complete the proof we need to show that $\mathcal{R}(K)$ is a dense subset of $\mathcal{K}$. To this end we assume that there is a function $v \in \mathcal{K}$ which is orthogonal to $\mathcal{R}(K)$. In this case we know from (13) that $K^* v = 0$, *i.e.*, that $v = 0$ on Γ_0. By Lemma 1.1 v also has vanishing Neumann values on Γ_0. The unique continuation property for harmonic functions (*cf.* [11]) therefore implies that $v = 0$ in $\Omega \setminus \Sigma$, and hence, $\mathcal{R}(K)$ is dense in $\mathcal{K}$. □

Theorem 2.2. *The difference $\tilde{\Lambda} - \Lambda : \mathrm{L}^2_\diamond(\Gamma_0) \to \mathrm{L}^2_\diamond(\Gamma_0)$ of the two Neumann-Dirichlet operators is a selfadjoint and positive semidefinite operator. As such, $\tilde{\Lambda} - \Lambda$ has a selfadjoint and positive semidefinite square root $(\tilde{\Lambda} - \Lambda)^{1/2}$, and a function $g \in \mathrm{L}^2_\diamond(\Gamma_0)$ belongs to the range of this square root operator, if and only if $g = \gamma_0 w$ for some harmonic function $w \in \mathrm{H}^1_\diamond(\Omega \setminus \Sigma)$ with*

$$\frac{\partial w}{\partial \nu} = 0 \quad \text{on } \Gamma \qquad \text{and} \qquad \left[\frac{\partial w}{\partial n}\right]_\Sigma = 0.$$

Proof. By virtue of (11) $\tilde{\Lambda} - \Lambda$ is selfadjoint and positive semidefinite, and following, for example, Proposition 2.18 in [5], its square root $(\tilde{\Lambda} - \Lambda)^{1/2}$ has range

$$\mathcal{R}((\tilde{\Lambda} - \Lambda)^{1/2}) = \mathcal{R}(K^*).$$

Thus, by Theorem 2.1, a function $g \in \mathrm{L}^2_\diamond(\Gamma_0)$ belongs to $\mathcal{R}((\tilde{\Lambda} - \Lambda)^{1/2})$, if and only if $g = \gamma_0 w$ for some $w \in \mathcal{K}$. The assertion now follows from Lemma 1.1. □

3. A test for cracks

Now we utilize Theorem 2.2 to search the domain Ω for cracks, similar to a reconstruction procedure suggested by Kirsch and Ritter [9] for an inverse scattering problem.

Consider a compact, simple arc $\Sigma_0 \subset \Omega$ and an associated double layer potential

$$v_1(x) = \frac{1}{2\pi} \int_{\Sigma_0} \frac{\partial}{\partial n(y)} \log \frac{1}{|x-y|} \varphi(y)\, \mathrm{d}s(y), \qquad x \in \Omega \setminus \Sigma_0, \tag{14}$$

with a smooth density φ which is positive except at the end points of the cracks where it vanishes Hölder continuously. It follows from [10, Th. 8.24] that $v_1 \in \mathrm{H}^1(\Omega \setminus \Sigma_0)$ and hence that we can determine a constant c such that $v_1 - c \in \mathrm{H}^1_\diamond(\Omega \setminus \Sigma_0)$. Next we investigate the boundary value problem

$$\Delta v_0 = 0 \quad \text{in } \Omega, \qquad \frac{\partial v_0}{\partial \nu} = \frac{\partial v_1}{\partial \nu} \quad \text{on } \Gamma. \tag{15}$$

According to the divergence theorem, and using the fact that v_1 is harmonic in $\Omega \setminus \Sigma_0$, we have

$$\int_\Gamma \frac{\partial v_1}{\partial \nu}\, \mathrm{d}s = \int_{\Omega \setminus \Sigma_0} \Delta v_1\, \mathrm{d}x - \int_{\Sigma_0} \left[\frac{\partial v_1}{\partial n}\right]_{\Sigma_0} \mathrm{d}s = -\int_{\Sigma_0} \left[\frac{\partial v_1}{\partial n}\right]_{\Sigma_0} \mathrm{d}s.$$

The final integral vanishes because $[\partial v_1/\partial n]_{\Sigma_0} = 0$ for the double-layer potential, *cf.* [10, Theorem 6.19]. This implies that the boundary value problem (15) has a unique solution $v_0 \in \mathrm{H}^1_\diamond(\Omega)$, and $v = v_1 - v_0 - c \in \mathrm{H}^1_\diamond(\Omega \setminus \Sigma)$ solves the diffraction problem

$$\Delta v = 0 \quad \text{in } \Omega \setminus \Sigma_0, \qquad \frac{\partial v}{\partial \nu} = 0 \quad \text{on } \Gamma, \qquad \left[\frac{\partial v}{\partial n}\right]_{\Sigma_0} = 0. \tag{16}$$

Theorem 3.1. *Let v be as above, and denote by $g_{\Sigma_0} = \gamma_0 v$ its boundary values on Γ_0. Then $g_{\Sigma_0} \in \mathcal{R}((\tilde{\Lambda} - \Lambda)^{1/2})$ if and only if $\Sigma_0 \subset \Sigma$.*

Proof. Assume first that $\Sigma_0 \subset \Sigma$. Then $\Omega \setminus \Sigma_0 \supset \Omega \setminus \Sigma$ and g_{Σ_0} belongs to the range of $(\tilde{\Lambda} - \Lambda)^{1/2}$ by virtue of (16) and Theorem 2.2.

On the other hand, if $g_{\Sigma_0} \in \mathcal{R}((\tilde{\Lambda} - \Lambda)^{1/2})$ then it follows from Theorem 2.2 that $g_{\Sigma_0} = \gamma_0 w$ for some harmonic function $w \in \mathrm{H}^1_\diamond(\Omega \setminus \Sigma)$ which satisfies (8). This implies that v of (16) and w have the same Neumann and Dirichlet values on Γ_0, and hence $v = w$ in $\Omega \setminus (\Sigma \cup \Sigma_0)$ according to the unique continuation property. Moreover, v can be extended to a harmonic function in $\Omega \setminus \Sigma$. On the other hand, the double-layer potential v has a nonzero jump across Σ_0, *cf.* [10, Theorem 6.17]. Therefore, we necessarily have $\Sigma_0 \subset \Sigma$. □

Remark 3.2. Theorem 3.1 gives rise to a constructive test whether some arc Σ_0 is part of Σ or not. We emphasize that for complete data, *i.e.*, when Γ_0 is the entire boundary of Ω, it is *not* necessary to solve the boundary value problem (15) to implement this test, because only the Dirichlet values of v_0 are required for the

computation. By definition, these Dirichlet values can be obtained from the local Neumann-Dirichlet operator for the Laplacian,

$$v_0|_\Gamma = \Lambda\left(\frac{\partial}{\partial\nu}v_1\big|_\Gamma\right).$$

We therefore only need to compute $v_1|_\Gamma$ and $\partial v_1/\partial\nu|_\Gamma$, and then have

$$g_{\Sigma_0} = v_1|_\Gamma - \Lambda\left(\frac{\partial}{\partial\nu}v_1\big|_\Gamma\right) - c, \tag{17}$$

where c is the constant which makes $g_{\Sigma_0} \in \mathrm{L}^2_\diamond(\Gamma)$.

4. Perfectly conducting cracks

Very similar results can be established when the cracks are perfectly conducting rather than insulating. In this case, the boundary current f yields a potential $\hat{u} \in \mathrm{H}^1_{\diamond,\Sigma}$ which solves the weak problem

$$\int_\Omega \operatorname{grad}\hat{u}\cdot\operatorname{grad}\hat{\phi}\,\mathrm{d}x = \int_{\Gamma_0} f\hat{\phi}\,\mathrm{d}s \qquad \text{for all } \hat{\phi}\in\mathrm{H}^1_{\diamond,\Sigma},$$

where $\mathrm{H}^1_{\diamond,\Sigma} \subset \mathrm{H}^1_\diamond(\Omega)$ is the set of all functions $\hat{\phi}\in\mathrm{H}^1_\diamond(\Omega)$ which are constant along each of the cracks in Σ. Denote by $\hat{\Lambda}$ the Neumann-Dirichlet operator which takes f and maps it onto $\hat{u}|_{\Gamma_0}$.

The orthogonal complement $\hat{\mathcal{K}}$ (with respect to the inner product (7)) of $\mathrm{H}^1_{\diamond,\Sigma}$ in $\mathrm{H}^1_\diamond(\Omega)$ consists of all harmonic functions w in $\Omega\setminus\Sigma$ with homogeneous Neumann data on Γ which satisfy

$$\int_\sigma \left[\frac{\partial w}{\partial n}\right]_\sigma \mathrm{d}s = 0 \qquad \text{for each crack } \sigma. \tag{18}$$

Note that (18) replaces the flux condition (8) in the definition of the subspace $\mathcal{K}$.

The results of Section 2 need some obvious modifications in the conducting case. The difference operator $\hat{\Lambda}-\Lambda$ is negative semidefinite and we have the normal equation type factorization

$$\Lambda - \hat{\Lambda} = \hat{K}^*\hat{K}, \qquad \hat{K}: \begin{cases} \mathrm{L}^2_\diamond(\Gamma_0) \longrightarrow \mathrm{H}^1_\diamond(\Omega), \\ f \longmapsto u - \hat{u}. \end{cases}$$

The range of $\hat{K}$ is dense in $\hat{\mathcal{K}}$ and $\hat{K}^*$ equals the trace operator on $\hat{\mathcal{K}}$. In other words, a function w belongs to $\mathcal{R}((\Lambda-\hat{\Lambda})^{1/2})$ if and only if it is the trace of some function $w\in\mathrm{H}^1_\diamond(\Omega)$, which is harmonic in $\Omega\setminus\Sigma$, satisfies (18), and has homogeneous Neumann values on Γ.

Because of the requirement $w\in\mathrm{H}^1_\diamond(\Omega)$ these functions are continuous across Σ, and hence, the double-layer potential v_1 in (14) can no longer serve to construct test functions as in Section 3. Instead we have to use a single-layer potential (with, *e.g.*, piecewise constant density φ) for v_1 in the conducting case,

$$v_1(x) = \frac{1}{2\pi}\int_{\Sigma_0}\log\frac{1}{|x-y|}\varphi(y)\,\mathrm{d}s(y), \qquad x\in\Omega\setminus\Sigma_0.$$

In order to construct v_0 as in (15) we require that φ satisfies the integrability condition

$$0 = \int_{\Sigma_0}\left[\frac{\partial v_1}{\partial n}\right]_{\Sigma_0}\mathrm{d}s = \int_{\Sigma_0}\varphi\,\mathrm{d}s,$$

where the last equality follows from the jump relation of the single-layer potential.

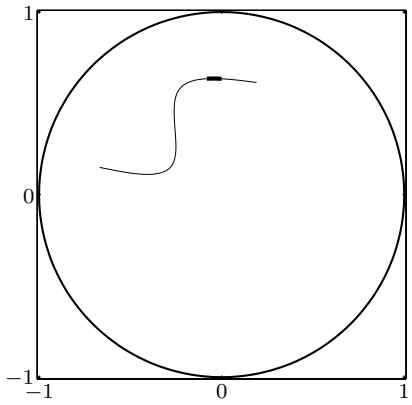

FIGURE 1. A crack phantom (thin line) and a test crack (thick line).

5. Numerical experiments

In practice we face the problem that a given arc Σ_0 will rarely lie exactly on an actual crack Σ. The best we can hope for is that g_{Σ_0} of (17) is "almost" contained in $\mathcal{R}((\tilde{\Lambda}-\Lambda)^{1/2})$ if the test crack Σ_0 is "almost" contained in Σ. To put this in concrete terms, we briefly review how the test whether $g \in \mathcal{R}((\tilde{\Lambda}-\Lambda)^{1/2})$ or not, has been accomplished numerically in [3]. Since $\tilde{\Lambda}-\Lambda$ is selfadjoint, positive semidefinite and compact there exists a countable set of nonnegative eigenvalues λ_j and eigenfunctions v_j such that

$$(\tilde{\Lambda}-\Lambda)f = \sum_{j=1}^{\infty} \lambda_j \langle f, v_j \rangle_{\mathrm{L}^2(\Gamma_0)} v_j.$$

Equipped with these prerequisites the Picard criterion yields the equivalence

$$g \in \mathcal{R}((\tilde{\Lambda}-\Lambda)^{1/2}) \qquad \text{if and only if} \qquad g \perp \mathcal{N}(\tilde{\Lambda}-\Lambda) \quad \text{and} \quad \sum_{j=1}^{\infty} \frac{\langle g, v_j \rangle^2_{\mathrm{L}^2(\Gamma_0)}}{\lambda_j} < \infty. \tag{19}$$

Numerical computations reveal an essentially geometric decay of the terms in the series (19); therefore we use a least squares fit to estimate a decay rate $1/\rho$ such that

$$\frac{\langle g, v_j \rangle^2_{\mathrm{L}^2(\Gamma_0)}}{\lambda_j} \sim \frac{1}{\rho^j}. \tag{20}$$

Accordingly we conclude that $g \in \mathcal{R}((\tilde{\Lambda}-\Lambda)^{1/2})$ if and only if $\rho > 1$, see [3] for more details.

In the sequel we present some numerical experiments based on simulated data using 255 trigonometric boundary currents. These were generated using a boundary integral method which requires the solution of a system of integral equations. One of these involves a hypersingular integral operator which can be discretized utilizing an idea of Mönch [12].

Before we show any numerical reconstructions we comment on the sensitivity of ρ with respect to the location of Σ_0 which is crucial for the performance of our algorithm. More specifically, we examine the sensitivity of ρ with respect to shifts and rotations of Σ_0. To this end we consider the crack phantom Σ shown in Figure 1 (the thin line) and a test crack $\Sigma_0 \subset \Sigma$ indicated by the thick line in Figure 1; we mention that Σ_0 is not a straight line. We move this test crack in the vertical direction, and for each position we determine the corresponding value of ρ. These numbers are drawn in Figure 2 (left) *versus* the amount of vertical shift. The label 0 at

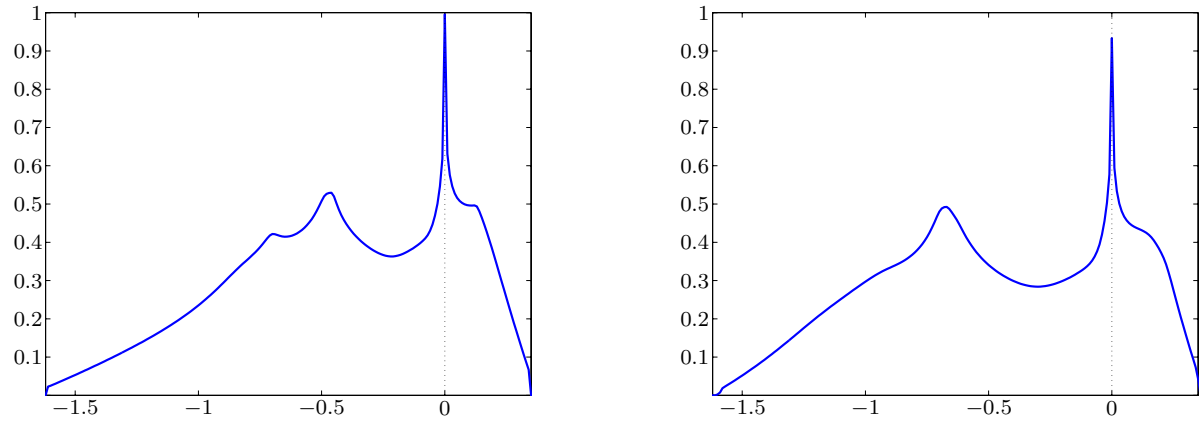

FIGURE 2. Decay rate ρ *vs.* vertical shift of test crack (left) and point dipole (right), respectively.

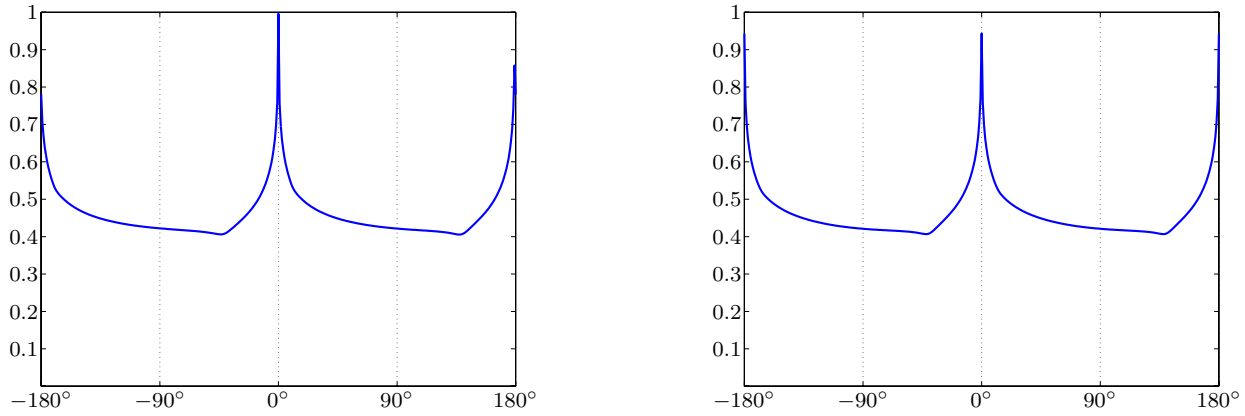

FIGURE 3. Decay rate ρ *vs.* rotation angle of test crack (left) and point dipole (right), respectively.

the horizontal axis marks the original position of the test crack, where $\Sigma_0 \subset \Sigma$. The sharp peak of the graph indicates a very high sensitivity of ρ with respect to displacements, and only for the zero shift does the decay rate approach the threshold $\rho = 1$.

For comparison we repeat this experiment with a "degenerated" crack which consists of only one single point and corresponds to a dipole singularity in this point. This degenerate case coincides exactly with the test for inclusions utilized in [3]. Note that the strong singularity of the dipole prevents the boundary values of the associated potential v from belonging to $\mathcal{R}((\tilde{\Lambda} - \Lambda)^{1/2})$, since $v \notin \mathrm{H}^1_\diamond(\Omega \setminus \Sigma)$. The results of these calculations are shown in Figure 2 (right). Apparently, the two plots are qualitatively very similar, the main difference being that in the degenerate case the peak fails to reach the threshold $\rho = 1$, as is consistent with the theory.

A similar experiment can be used to study the dependence of ρ on the orientation of the test crack. To this end we rotate Σ_0 shown in Figure 1 around its center point. The corresponding numbers for ρ are displayed in Figure 3 (left). As before, the right hand side plot corresponds to a test with a dipole on the actual crack Σ but with rotating dipole axis. Again, the two figures are very similar and exhibit the strong sensitivity of ρ.

These experiments show that both kinds of test functions are feasible for the localization of cracks provided that the test is based on an appropriate threshold level for ρ. On the other hand, the sharp peaks in the figures make clear that a very fine grid of test points is necessary to achieve good reconstructions.

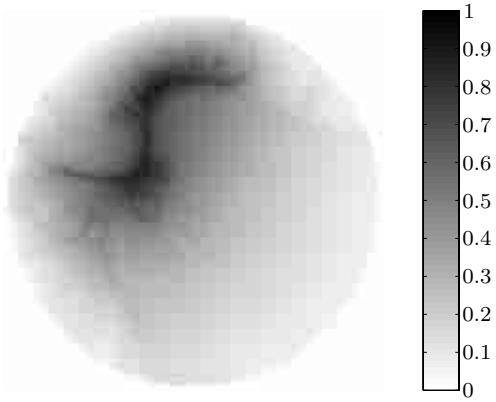

FIGURE 4. Reconstruction of the crack phantom.

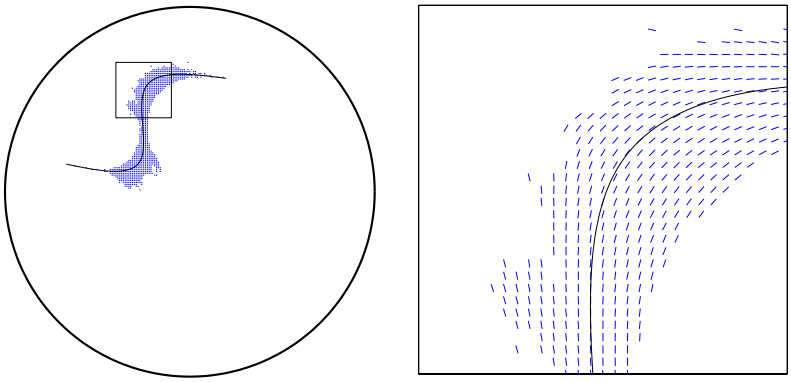

FIGURE 5. Points with $\rho > 0.75$ and corresponding dipole axes.

The result of such a grid search is shown in Figure 4. In this case the grid is an equidistant square mesh with mesh width 0.01. For each of the 3165 grid points within the disk and each of 100 equi-angled dipole axes we compute the test function of the corresponding point dipole and its associated value ρ, *i.e.* for each grid point we perform the same calculations as for Figure 3 (right). The maximum of these values of ρ is assigned to this point as a grayscale value, and from this the plot in Figure 4 is obtained. The crack is well reconstructed by this procedure although there occur some artefacts near the crack.

As another means of visualization Figure 5 shows the crack phantom and contains for all grid points with $\rho > 0.75$ the corresponding dipole axis for which the maximum was attained. The zoom on the right demonstrates that these dipole axes are nicely aligned with the actual crack.

A further example shows the reconstruction of two cracks, *cf.* Figure 6. We emphasize that *a priori* knowledge about the number of cracks is not required in advance.

6. CONCLUSIONS

In this work we developed a characterization of cracks in a similar manner as in the case of inclusions [2, 3]. The use of the factorizaton (11) rather than an analog of (10) simplifies the subsequent analysis substantially. However, the fact that a crack carries a directional information incorporates an additional dimension to the

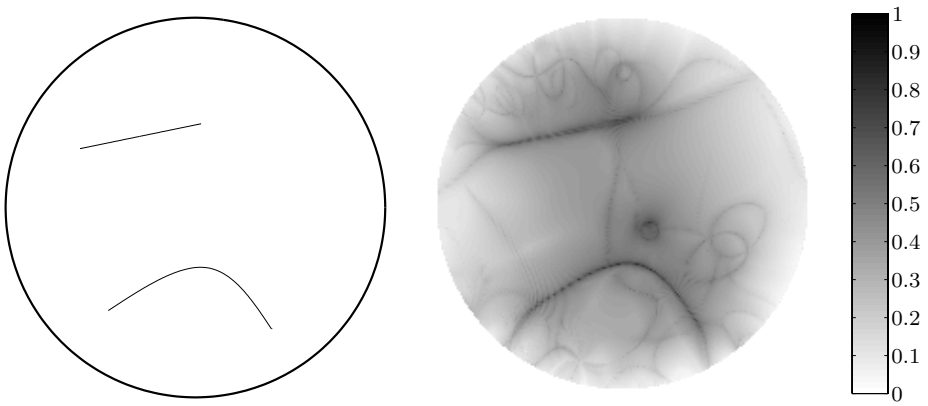

FIGURE 6. Reconstruction of two cracks.

reconstruction in the inverse problem. For this reason the numerical realization of our method is significantly more expensive than in the case of inclusions and forms a real computational challenge.

Acknowledgements. We would like to thank Andreas Kirsch for his careful reading of the manuscript.

REFERENCES

[1] G. Alessandrini and A. Diaz Valenzuela, Unique determination of multiple cracks by two measurements. *SIAM J. Control Optim.* **34** (1996) 913–921.
[2] M. Brühl, Explicit characterization of inclusions in electrical impedance tomography. *SIAM J. Math. Anal.* **32** (2001) 1327–1341.
[3] M. Brühl and M. Hanke, Numerical implementation of two noniterative methods for locating inclusions by impedance tomography. *Inverse Problems* **16** (2000) 1029–1042.
[4] K. Bryan and M. Vogelius, A computational algorithm to determine crack locations from electrostatic boundary measurements. The case of multiple cracks. *Internat. J. Engrg. Sci.* **32** (1994) 579–603.
[5] H. W. Engl, M. Hanke and A. Neubauer, *Regularization of inverse problems*. Kluwer, Dordrecht (1996).
[6] A. Friedman and M. Vogelius, Determining cracks by boundary measurements. *Indiana Univ. Math. J.* **38** (1989) 527–556.
[7] H. Kim and J. K. Seo, Unique determination of a collection of a finite number of cracks from two boundary measurements. *SIAM J. Math. Anal.* **27** (1996) 1336–1340.
[8] A. Kirsch, Characterization of the shape of a scattering obstacle using the spectral data of the far field operator. *Inverse Problems* **14** (1998) 1489–1512.
[9] A. Kirsch and S. Ritter, A linear sampling method for inverse scattering from an open arc. *Inverse Problems* **16** (2000) 89–105.
[10] R. Kreß, *Linear integral equations*. 2nd edn., Springer, New York (1999).
[11] C. Miranda, *Partial differential equations of elliptic type*. 2nd edn., Springer, Berlin (1970).
[12] L. Mönch, On the numerical solution of the direct scattering problem for an open sound-hard arc. *J. Comput. Appl. Math.* **71** (1996) 343–356.
[13] N. Nishimura and S. Kobayashi, A boundary integral equation method for an inverse problem related to crack detection. *Internat. J. Numer. Methods Engrg.* **32** (1991) 1371–1387.
[14] F. Santosa and M. Vogelius, A computational algorithm to determine cracks from electrostatic boundary measurements. *Internat. J. Engrg. Sci.* **29** (1991) 917–937.